




Cite this: *Phys. Chem. Chem. Phys.*,  
2024, 26, 19845

Received 29th May 2024,  
Accepted 1st July 2024

DOI: 10.1039/d4cp02207f

rsc.li/pccp

# Water-assisted absorption of CO<sub>2</sub> by 3-amino-1-propanol: a mechanistic insight†

Shivam Rawat and C. N. Ramachandran \*

The mechanism of the proton transfer in the reaction between CO<sub>2</sub> and 3-amino-1-propanol with and without water molecules is investigated quantum-mechanically. Studies revealed that water molecules and the hydroxy group of 3-amino-1-propanol explicitly participate in the proton transfer, forming carbamic acid. It is found that water has a high impact on the energetics of CO<sub>2</sub> absorption by reducing the barrier for proton transfer. Apart from the water molecules, the hydroxy group of alkanolamine significantly affects the energetics of the reaction. Five cases involving two, three, and four protons are discussed, and it is found that the proton transfer occurs in a concerted manner that depends on the initial configuration of the reaction complex. The present study unequivocally confirms the role of water molecules in the CO<sub>2</sub> capturing *via* amine-based solvents.

## 1. Introduction

In recent years, there has been growing interest in CO<sub>2</sub> capture and storage (CCS). It comprises separating CO<sub>2</sub> from the flue gas after combustion, followed by the transport and storage.<sup>1</sup> Post-combustion CO<sub>2</sub> capture (PCC) based on amines and their derivatives is one of the most exploited CCS methods.<sup>2</sup> The major advantage of PCC is that it can be retrofitted to the existing infrastructure, which reduces the cost of implementation. This technology is renowned for its capacity to facilitate reversible reactions with CO<sub>2</sub> and is currently considered as the most viable and economically efficient approach.<sup>1–7</sup> Amines, especially alkanolamines, have been widely used for natural gas processing competently performed in PCC plants. It is well-known that the nitrogen atom of the amine group has an affinity towards CO<sub>2</sub>, which has been exploited in the PCC process. However, an understanding of the reaction mechanism is required to enhance the efficiency of the capturing process. Several mechanisms have been proposed for the reaction between CO<sub>2</sub> and amines. The zwitterion mechanism, termolecular mechanism, and carbamic acid mechanism are prominently known mechanisms.<sup>8–11</sup>

The zwitterion mechanism is a two-step mechanism shown in steps 1 and 2 of the scheme below. In the first step, a protonated carbamate zwitterion intermediate is formed with the formation of a bond between the carbon atom of CO<sub>2</sub> and the nitrogen atom of amine. In the next step, the base extracts the extra proton in the protonated carbamate ion,

forming carbamate.<sup>8,9</sup> At a low CO<sub>2</sub> loading, the carbamate concentration is low, making the reaction irreversible; deprotonation of the zwitterion is the rate-determining step.

The termolecular reaction mechanism is similar to the zwitterion mechanism, except that it occurs in a single step 3, as shown in the scheme below. The formation of a bond occurs when the nitrogen atom of the amine interacts with the carbon atom of CO<sub>2</sub>. This interaction is accompanied by the simultaneous transfer of a proton from the nitrogen of the amino group to the adjacent molecule of the base.<sup>10</sup> According to the carbamic acid mechanism, the proton of the amine group is instantaneously migrated to one of the oxygen atoms of the carboxylate group, forming carbamic acid, followed by the proton abstraction to form a carbamate ion<sup>11</sup> shown as steps 4 and 5 of Scheme 1.

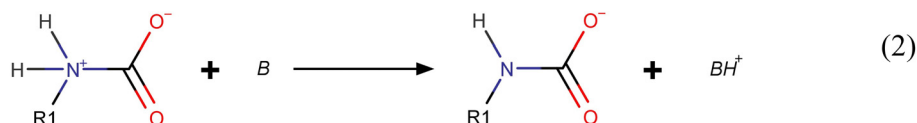
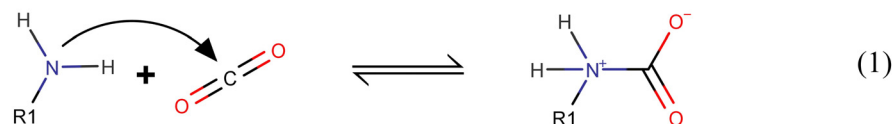
The mechanisms discussed above are still a topic of debate among the research communities working in this field. The reactions involved in the process of CO<sub>2</sub> absorption *via* amines and their derivatives are kinetically fast and it is difficult to probe into the process experimentally.<sup>7</sup> Therefore, computational methods are applied for such investigations. Various studies have been reported to find the mechanistic details of the reaction between CO<sub>2</sub> and aqueous amines as well as their derivatives using quantum mechanical methods.<sup>12–21</sup>

Yamada *et al.* studied CO<sub>2</sub> absorption in aqueous alkanolamine solutions, including the effect of the alkyl chain length and revealed that intramolecular hydrogen bonds play a crucial role.<sup>22,23</sup> However, these studies did not consider the effect of explicit water molecules.<sup>22</sup> Ismael *et al.* theoretically investigated the reaction between CO<sub>2</sub> and 2-amino-2-methyl-1-propanol (AMP) in the presence of explicit water molecules.<sup>24</sup> Their studies revealed that the AMP-CO<sub>2</sub>-H<sub>2</sub>O ternary complex follows a single-step, third-order reaction mechanism. Sunkyung *et al.*

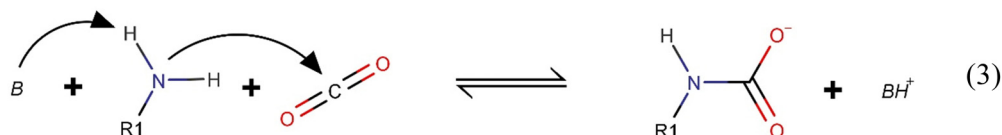
Department of Chemistry, Indian Institute of Technology Roorkee, Roorkee, Uttarakhand 247667, India. E-mail: ramcn@cy.iitr.ac.in

† Electronic supplementary information (ESI) available. See DOI: <https://doi.org/10.1039/d4cp02207f>

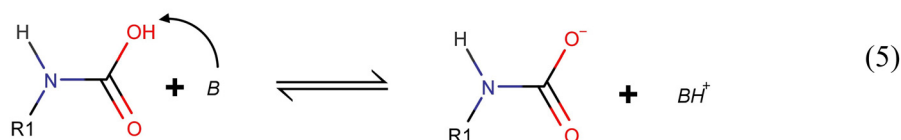
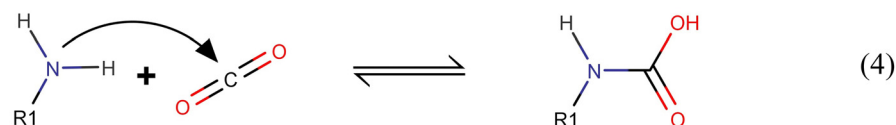
## a. Zwitterion mechanism



## b. Termolecular mechanism



## c. Carbamic acid mechanism

Scheme 1 Different types of mechanisms proposed for CO<sub>2</sub> absorption via amines.

quantum mechanically studied the mechanism of CO<sub>2</sub> absorption *via* amines and the carbamate formation using an additional amine as a base, and this has been validated as the more plausible model compared to other proposed mechanisms.<sup>25</sup> Studies revealed that the reactants with explicit water molecules are critical for investigating the reaction. However, the involvement of the additional functional groups, such as the hydroxy group in alkanolamines, has not been well examined. It is intuitive to determine whether the alkanolamines' proton of the hydroxy group also participates in the proton transfer. Aso *et al.* studied the reaction mechanism involving 2-(2-aminoethyl-amino)ethanol, CO<sub>2</sub>, and water, in which they showed that the proton of the hydroxy group is involved in the proton transfer.<sup>26</sup> However, their study was limited to proton transfer involving only one water molecule and did not consider the effect of more than one water molecule in the process. Said *et al.* found evidence for the water-assisted CO<sub>2</sub> absorption *via* amines in their combined experimental and computational studies.<sup>27</sup> Using isotopic

methods, they examined the role of water in the formation of carbamic acid, revealing that the deuterium of water is shifted to carbamic acid. In contrast, the theoretical results supported the formation of carbamic acid as a more favorable one when assisted by amines compared to that assisted by water. However, their studies were limited to amines and single water molecules, suggesting the need for further investigation. In the present study, we examine the reaction between 3-amino-1-propanol (3A1P) and CO<sub>2</sub> in the presence and absence of explicit water molecules. A comparison of proton transfer with and without the involvement of the hydroxy proton is also carried out.

## 2. Computational methodology

All the quantum mechanical calculations are carried out using the Gaussian09 program.<sup>28</sup> For the calculations, the M06-2X functional and cc-pVDZ basis sets are used.<sup>29,30</sup> The M06-2X functional is selected because it effectively describes interactions

between the molecules in which non-covalent interactions are present.<sup>31</sup> Solvent effects due to water are investigated using the integral equation formalism polarizable continuum model (IEF-PCM). The Gibbs free energies of reactants, intermediates, transition states, and products are determined using the same computational approach. All the reactant complexes (RCs), intermediates (IMs), and product complexes (PCs) are confirmed at the minima of the respective potential surface, indicated by the absence of imaginary frequencies obtained from the Hessian calculations. A fine numerical integration grid (75,302 grid) together with default convergence criteria (maximum force  $4.5 \times 10^{-4}$ , maximum displacement  $1.8 \times 10^{-3}$ , and energy  $10^{-6}$  a.u.) are used. The Gibbs free energy for all the species is calculated at 298 K and 1 atm pressure. The transition states are searched using the synchronous transit-guided quasi-Newton (STQN) method.<sup>32</sup> The transition states are identified by detecting a single imaginary frequency and subsequently validated through intrinsic reaction coordinate calculations. Natural bond orbital (NBO) analysis is carried out for the transition state involving the proton transfer to gain insights into various types of interactions present in the system.<sup>33</sup> Bond critical point analysis has been done using Multiwfn software.<sup>34,35</sup> The visualization of bond critical points is done using VMD software.<sup>36</sup>

### 3. Results and discussion

The mechanistic study investigates the absorption of CO<sub>2</sub> and the formation of carbamic acid *via* the shifting of protons in a concerted manner with and without the direct involvement of water molecules. Three different types of reactant complexes (RCs) are considered according to their chemical composition, and are further classified into five different configurations, *i.e.* (i) CO<sub>2</sub>-3A1P involving two proton transfer, (ii) CO<sub>2</sub>-3A1P-H<sub>2</sub>O involving two proton transfer, (iii) CO<sub>2</sub>-3A1P-H<sub>2</sub>O involving three proton transfer, (iv) CO<sub>2</sub>-3A1P-2H<sub>2</sub>O involving three

proton transfer, and (v) CO<sub>2</sub>-3A1P-2H<sub>2</sub>O involving four proton transfer. The free energy profile for the reactions of the above cases is provided in Fig. 1 and 2. The number of water molecules and the number of protons involved in different cases mentioned above are summarized in Table 1.

In case (i), which involves CO<sub>2</sub>-3A1P without any explicit water molecules, the reaction proceeds in two steps, as depicted in Fig. S1 of the ESI.† The distance between the carbon of CO<sub>2</sub> and nitrogen of 3A1P in the reactant complex (RC) is 2.86 Å. This suggests a weak interaction between the two reactant species. However, there is a strong interaction between the proton of the hydroxy group and the nitrogen of 3A1P that gets decreased due to the interaction of CO<sub>2</sub> with 3A1P. The binding of CO<sub>2</sub> with the nitrogen atom forms a protonated carbamate ion intermediate (IM). As a result, the C–N internuclear distance is reduced to 1.62 Å. The energy of the IM is 6.9 kcal mol<sup>−1</sup> higher than that of the RC, suggesting that the formation of an intermediate is not favoured without the involvement of water molecules. This is consistent with the results of Said *et al.*, where it is reported that the 1,3-zwitterion formation *via* a four-membered transition state is unfavorable.<sup>27</sup> The next step involves the formation of carbamic acid *via* proton transfer. The proton of the amino group is transferred to the hydroxy group, and the proton of the hydroxy group is transferred to the carboxylate group in a concerted way through a six-membered transition state TS2, as shown in Fig. S1 of the ESI.† The product complex (PC) is ultimately formed from the transition state TS2. The energy barrier for the proton transfer is 10.7 kcal mol<sup>−1</sup>, which is the rate-determining step of the reaction.

Although the above study was carried out in an aqueous environment using the implicit solvent model, the water molecule was not explicitly present. Considering the fact that in an aqueous solvent, water is omnipresent, we examined the effect of an explicit water molecule on the mechanism of the reaction, as illustrated in Fig. S2 of the ESI.† However, the addition of

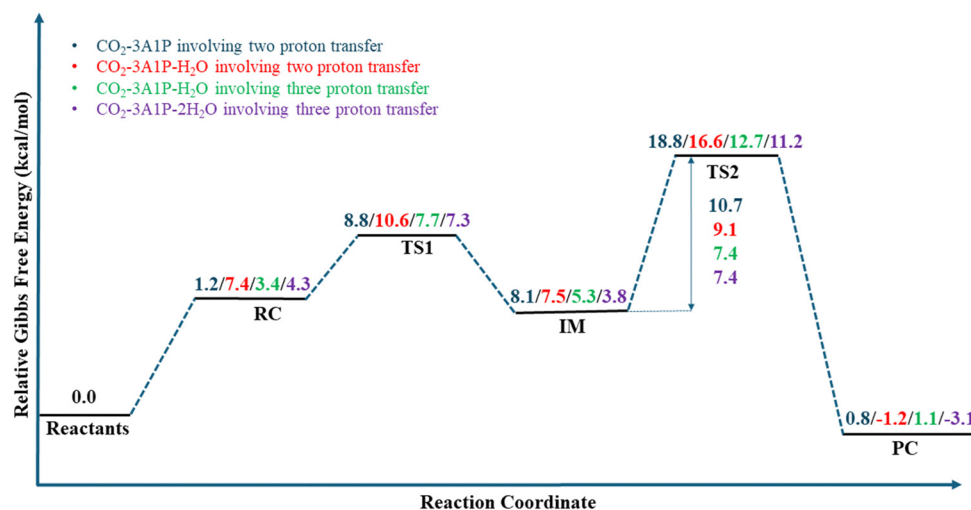


Fig. 1 Schematic diagram showing the Gibbs free energy change associated with CO<sub>2</sub> absorption by 3-amino-1-propanol in the presence of different numbers of water molecules, which follow a two-step mechanism.

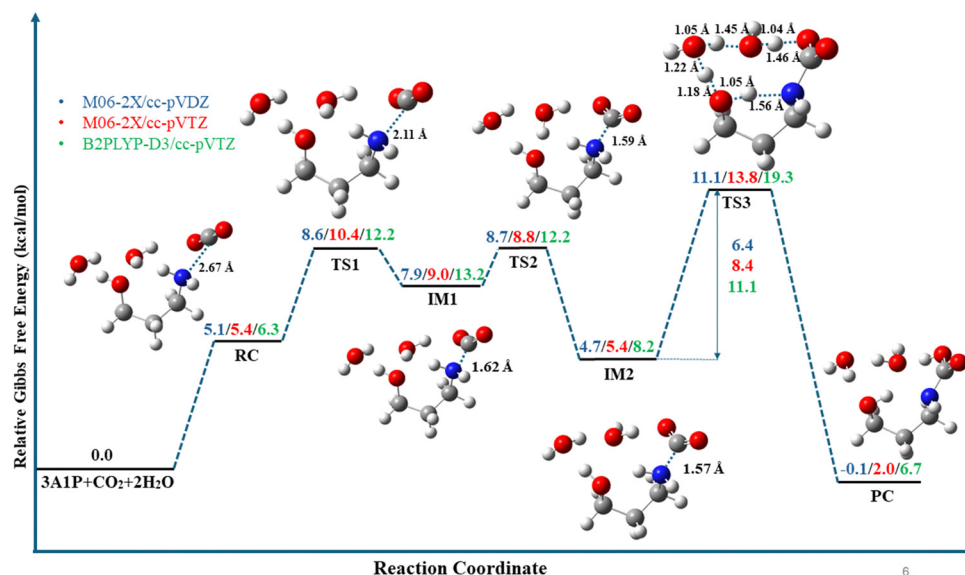


Fig. 2 The mechanism and the energy profile diagram for the CO<sub>2</sub> absorption using 3-amino-1-propanol in the presence of two water molecules involving four proton transfer. The optimized geometries obtained at M06-2X/cc-pVDZ are used for the single point energy calculations at M06-2X/cc-pVTZ and B2PLYP-D3/cc-pVTZ levels.

**Table 1** Interaction distance between the nitrogen of 3A1P and the carbon of CO<sub>2</sub> for various species involved in the reaction along with the associated Gibbs free energy change for the proton transfer step

Number of water molecules involved	Number of protons involved	RC (Å)	IM (Å)	PC (Å)	ΔG (kcal mol <sup>-1</sup> )
0	2	2.86	1.62	1.37	10.7
1	2	2.68	1.59	1.36	9.1
	3	2.85	1.59	1.40	7.4
2	3	2.66	1.59	1.38	7.4
	4	2.67	IM1 1.62 IM2 1.57	1.40	6.4

water molecules did not make any change in the mechanism of the reaction and the energy barrier because the proton transfer remained nearly the same.

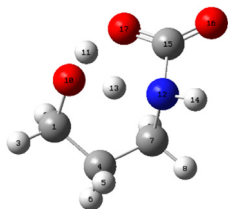
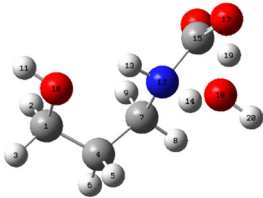
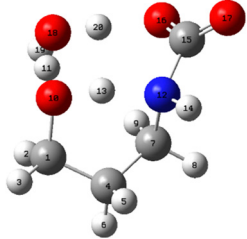

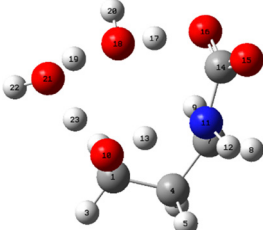
In the presence of one water molecule, the reaction occurs in two paths, namely case (ii) and case (iii), as depicted in Fig. S3 and S4 of the ESI.† In case (ii), the hydroxy group of 3-amino-1-propanol is not involved in the reaction, whereas in case (iii), the hydroxy group participates. The involvement of the hydroxy group depends on the orientation of water molecules around 3A1P in the RC. In case (ii), the C–N distance of 2.68 Å of RC is reduced to 1.59 Å on forming an IM (Fig. S3, ESI†). The relatively less energy difference between the RC and IM of the above, compared to that of case (i) can be attributed to the formation of a six-membered cyclic transition state TS1. In the rate-determining step of case (ii), two protons are transferred. The transition state for the formation of carbamic acid is depicted as TS2 in Fig. S3 of the ESI.† From the transition state structure, it is evident that the extra proton in the amine group of the protonated carbamate ion intermediate is transferred to the oxygen atom of the water molecule. Subsequently, the proton of the water molecule is transferred to the oxygen atom of the carboxylate group in a concerted manner.

The Gibbs free energy of activation for the rate-determining step of case (ii) is found to be 9.1 kcal mol<sup>-1</sup>, which is less than that observed for case (i). Thus, it can be inferred that the participation of water molecules makes the proton transfer more feasible.

In the RC of case (iii), the proton of the hydroxy group of 3A1P interacts with the water molecule, as depicted in Fig. S4 (ESI†). After the absorption of CO<sub>2</sub>, the distance between C and N is reduced from 2.85 Å to 1.59 Å. In the next step, the proton that binds to the nitrogen atom is transferred to oxygen of the hydroxy group. Subsequently, the proton of the hydroxy group is transferred to the oxygen atom of the water molecule. This is followed by shifting of the proton of the water molecule towards the carboxylate group, forming a product complex. The Gibbs free energy of activation for the rate-determining step is 7.4 kcal mol<sup>-1</sup>, which is less compared to those of previous two cases. This suggests that apart from the water molecule, the involvement of the hydroxy group also facilitates the proton transfer.

Two cases are studied for the proton transfer involving two water molecules. Among these two cases (case (iv) and (v)), the hydroxy group of 3A1P does not participate in the proton

**Table 2** Natural bond orbital analysis of the transition states involving the proton transfer

Case	Transition state	NBO donor	NBO acceptor	$\Delta E_{ij}^{(2)}$ (kcal mol <sup>-1</sup> )
(i)		LP (N <sub>12</sub> )	$\sigma^*$ (O <sub>10</sub> H <sub>13</sub> )	139
		LP (O <sub>17</sub> )	$\sigma^*$ (O <sub>10</sub> H <sub>11</sub> )	123
(ii)		LP (N <sub>12</sub> )	$\sigma^*$ (O <sub>18</sub> H <sub>14</sub> )	137
		LP (O <sub>17</sub> )	$\sigma^*$ (O <sub>18</sub> H <sub>19</sub> )	144
(iii)		LP (N <sub>12</sub> )	$\sigma^*$ (O <sub>10</sub> H <sub>13</sub> )	98
		LP (O <sub>16</sub> )	$\sigma^*$ (O <sub>18</sub> H <sub>20</sub> )	83
		LP (O <sub>18</sub> )	$\sigma^*$ (O <sub>10</sub> H <sub>11</sub> )	109
(iv)		LP (N <sub>12</sub> )	$\sigma^*$ (O <sub>21</sub> H <sub>14</sub> )	125
		LP (O <sub>17</sub> )	$\sigma^*$ (O <sub>18</sub> H <sub>19</sub> )	103
		LP (O <sub>18</sub> )	$\sigma^*$ (O <sub>21</sub> H <sub>23</sub> )	145
		$\sigma^*$ (O <sub>21</sub> H <sub>14</sub> )	$\sigma^*$ (O <sub>21</sub> H <sub>23</sub> )	13
		$\sigma$ (O <sub>18</sub> H <sub>19</sub> )	$\sigma^*$ (O <sub>21</sub> H <sub>23</sub> )	14
(v)		LP (N <sub>11</sub> )	$\sigma^*$ (O <sub>10</sub> H <sub>13</sub> )	65
		LP (O <sub>16</sub> )	$\sigma^*$ (O <sub>18</sub> H <sub>17</sub> )	83
		LP (O <sub>18</sub> )	$\sigma^*$ (O <sub>21</sub> H <sub>19</sub> )	79
		LP (O <sub>21</sub> )	$\sigma^*$ (O <sub>10</sub> H <sub>23</sub> )	187
		$\sigma$ (O <sub>21</sub> H <sub>19</sub> )	$\sigma^*$ (O <sub>10</sub> H <sub>23</sub> )	19

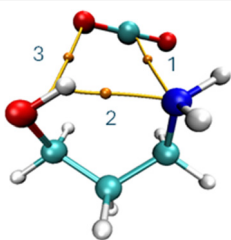
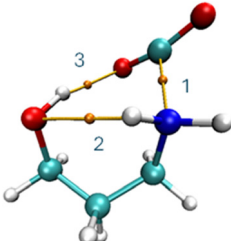
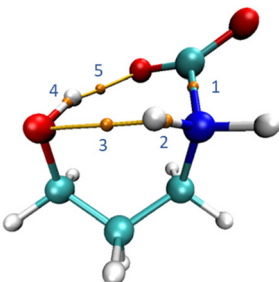
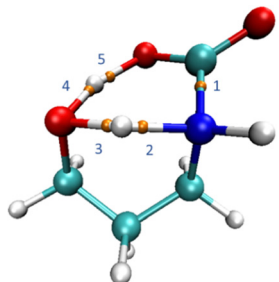
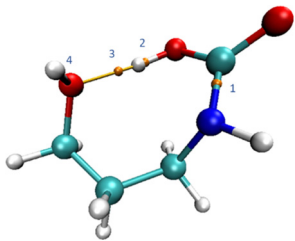
transfer in the first one, whereas it does in the second one. The mechanism and the energy profiles of case (iv) are depicted in Fig. S5 (ESI<sup>†</sup>) and of case (v) are provided in Fig. 2.

In case (iv), the distance between the nitrogen atom of 3A1P and the carbon atom of CO<sub>2</sub> is reduced from 2.66 Å to 1.59 Å, when the reactants are converted to the intermediate. In the next step, the above intermediate is converted to a product complex *via* the transition state TS2. During this transition, the additional proton residing on the nitrogen atom of the carbamate ion intermediate (IM) shifts to the oxygen atom of the first water molecule. This is accompanied by the transfer of one of the hydrogens of the first water molecule to the oxygen atom of the second water molecule. Concurrently, one of the hydrogens of the second water molecule is transferred to the oxygen atom of the carboxylate group in a concerted manner. The Gibbs free

energy of activation for the above step is 7.4 kcal mol<sup>-1</sup>, which is the rate-determining step.

As mentioned earlier, for case (v), the hydroxy group along with two water molecules participate in the proton transfer. The mechanism of the above reaction consists of three steps. In the first step, CO<sub>2</sub> is absorbed by nitrogen of 3A1P forming IM1. In the second step, IM1 is converted to IM2, during which the N–C bond distance is reduced from 1.62 Å to 1.57 Å. During this transition, one of the water molecules that interacts with the oxygen atom of the hydroxy group is rotated. As a result, the interaction of this water molecule with the hydroxy group is reduced. Subsequently, the intramolecular interaction between the –NH and –OH groups is enhanced, which is confirmed by the bond critical point analysis. In the next step of the reaction, IM2 is converted to a product complex *via* the transition state TS3.

**Table 3** The electron density ( $\rho$ ) and Laplacian of electron density ( $\nabla^2(\rho)$ ) at relevant (3,−1) critical points for the species involved in the proton transfer of CO<sub>2</sub>-3A1P

Species	Figure	Critical point	Atoms involved	Electron density ( $e/a_0^3$ )	Laplacian of electron density ( $e/a_0^5$ )
RC		1	N-C <sub>CO2</sub>	0.012	0.044
		2	H <sub>OH</sub> -N	0.028	0.083
		3	H <sub>OH</sub> -O <sub>CO2</sub>	0.010	0.039
TS1		1	N-C <sub>CO2</sub>	0.063	0.104
		2	H <sub>N</sub> -O <sub>OH</sub>	0.014	0.052
		3	H <sub>OH</sub> -O <sub>CO2</sub>	0.023	0.084
IM		1	N-C <sub>CO2</sub>	0.185	−0.196
		2	H <sub>N</sub> -N	0.320	−1.552
		3	H <sub>N</sub> -O <sub>OH</sub>	0.020	0.066
		4	H <sub>OH</sub> -O <sub>OH</sub>	0.332	−2.218
		5	H <sub>OH</sub> -O <sub>CO2</sub>	0.035	0.123
TS2		1	N-C <sub>CO2</sub>	0.253	−0.582
		2	H <sub>N</sub> -N	0.144	−0.233
		3	H <sub>N</sub> -O <sub>OH</sub>	0.180	−0.343
		4	H <sub>OH</sub> -O <sub>OH</sub>	0.216	−0.665
		5	H <sub>OH</sub> -O <sub>CO2</sub>	0.120	−0.013
PC		1	N-C <sub>CO2</sub>	0.318	−1.034
		2	O <sub>CO2</sub> -H <sub>CO2</sub>	0.343	−2.203
		3	O <sub>OH</sub> -H <sub>CO2</sub>	0.047	0.156
		4	O <sub>OH</sub> -H <sub>OH</sub>	0.312	−2.088

Four protons are involved in this concerted process, as illustrated in Fig. 2. In this process, the proton of the amine group is transferred to the oxygen atom of the hydroxy group, and the proton of the hydroxy group relocates to the oxygen atom of the first water molecule, followed by the transfer of its hydrogen atom to oxygen of the second water molecule. Simultaneously, one of the hydrogen atoms of the second water molecule is shifted toward the carboxylate group. The Gibbs free energy of activation for the concerted proton transfer step is 6.4 kcal mol<sup>−1</sup>, and is the

lowest among all the cases considered. From the change in Gibbs free energy value associated with the proton transfer for all the above cases (Table 1), it is concluded that among the proton transfer mechanisms, the one involving four protons is energetically the most favorable for CO<sub>2</sub> absorption.

The transition state corresponding to the proton transfer for all the cases is further investigated using the NBO analysis. The major interactions that lead to proton transfer are investigated and summarized in Table 2. From the table, it can be seen that



there are two major interactions present in case (i) *i.e.* LP ( $N_{12}$ )  $\rightarrow$   $\sigma^*$  ( $O_{10}H_{13}$ ) and LP( $O_{17}$ )  $\rightarrow$   $\sigma^*$  ( $O_{10}H_{11}$ ) with interaction energies of 139 kcal mol<sup>-1</sup> and 123 kcal mol<sup>-1</sup>, respectively. The interaction LP ( $N_{12}$ )  $\rightarrow$   $\sigma^*$  ( $O_{10}H_{13}$ ) leads to the transfer of the lone pair of electrons of the nitrogen atom to the antibonding orbital of the  $O_{10}H_{13}$  bond, leading to its elongation, suggesting less favorable transfer of  $H_{13}$  from  $N_{12}$  to  $O_{10}$ . On the other hand, in the interaction LP( $O_{17}$ )  $\rightarrow$   $\sigma^*$  ( $O_{10}H_{11}$ ), the lone pair electrons of  $O_{17}$  are transferred to the antibonding orbital of the  $O_{10}H_{11}$  bond, leading to the lengthening of the  $O_{10}H_{11}$  bond, thereby favoring the transfer of  $H_{11}$  to  $O_{17}$ . Out of these two interactions, the former is favored, and the latter one is less favored resulting in a relatively high energy barrier for the proton transfer. A similar observation is also made for case (ii), for which the favorable interaction is relatively even stronger than that in case (i). From the table, we can see that more such favorable interactions are present for the cases in which the number of protons transferred is more (case (iii) to case (v)). More details about these interactions are provided in Table S1 of the ESI.<sup>†</sup> The presence of more numbers of such favorable interactions as we move from case (i) to case (v) supports the consistent lowering of the energy barrier for the proton transfer.

To gain more insights into the energetics of various species, bond critical point (BCP) analysis that provides the topological features of electron density for the species involved in the reaction has been carried out. For this purpose, the electron density ( $\rho$ ) and Laplacian of electron density ( $\nabla^2(\rho)$ ) at bond critical points are determined as mentioned earlier. The values of  $\rho$  and  $\nabla^2(\rho)$  at the relevant (3, -1) bond critical points for the species involved in the proton transfer of  $CO_2$ -3A1P are provided in Table 3. For other systems, the above values are given in Table S2 of the ESI.<sup>†</sup>

It can be seen that the energy difference between the species involved in a reaction (reactant complex, transition states, intermediates, *etc.*) can be correlated with the change in electron density at different bond critical points of those species. For example, in Table 3, as we move from RC to TS1, it can be seen that the  $CO_2$  interaction with the amino group is increased, as reflected from the increase in the electron density at the critical point 1 ( $N-C_{CO_2}$ ) from 0.012 a.u. to 0.063 a.u. However, the electron density at the  $H_{OH}-N$  bond critical point in the RC disappears on forming TS1, although a marginal electron density is developed between  $H_N-O_{OH}$  for TS1. Thus, the higher energy of TS1 can be attributed to the disappearance of the strong interaction between the lone pair electrons of nitrogen and the hydrogen of the hydroxyl group. In IM1, the stabilization is due to the increased electron density at critical point 1 ( $N-C_{CO_2}$ ) from 0.063 a.u. to 0.185 a.u. Compared to the energy of IM1, that of TS2 is increased and can be attributed mainly to the decrement of the electron density at (3, -1) bond critical points  $H_{OH}-O_{OH}$  and  $H_N-N$  inducing the proton transfer. Finally, the energy is significantly reduced with the formation of PC due to the bond formation between  $N-C_{CO_2}$ ,  $O_{CO_2}-H_{CO_2}$  and  $O_{OH}-H_{OH}$  as evident from the electron density and the respective Laplacian of electron densities. A similar analysis

holds true for other systems as evident from Table S2 of the ESI.<sup>†</sup>

To know the effect of the basis set on the free energy barrier for the proton transfer, single point energy calculations were carried out at the M06-2X/cc-pVTZ level. The thermal correction to the electronic energy and the optimized geometries for this purpose were taken from the results obtained at the M06-2X/cc-pVDZ level. The energy profiles for various cases of the reaction are provided in Fig. 2 and Fig. S1–S5 of the ESI.<sup>†</sup> From the analysis, it was found that the energy barrier for the proton transfer decreases with the number of water molecules, irrespective of the basis sets used.

In addition, the effect of the functional on the energetics of the reaction is also examined using Grimme's D3BJ dispersion-corrected double hybrid functional B2PLYP-D3 with the cc-pVTZ basis set.<sup>37,38</sup> The thermal correction to the electronic energy and the optimized geometries for this purpose were taken from the results obtained at the M06-2X/cc-pVDZ level, as was done above. The results of these calculations are also incorporated in Fig. 2 and Fig. S1–S5 (ESI<sup>†</sup>). It is observed that the conclusion drawn on the barrier of the reaction to the number of water molecules did not change with the functional used.

## 4. Conclusion

The effect of water molecules and the hydroxy group of alkanolamine in the process of  $CO_2$  absorption *via* aqueous 3-amino-1-propanol is investigated. Five reaction paths have been analyzed according to the spatial arrangement of constituent molecules. The spatial orientation of the water molecules, as well as the number of water molecules involved in the reaction complex during the reaction, determine the mechanistic paths. The availability of a hydroxy group in the periphery of the alkanolamine–water complex significantly impacts the energetics of the formation of carbamic acid. The proton abstraction from the protonated carbamate ion is an essential step in the reaction between  $CO_2$  and 3A1P. Water as a solvent, not only stabilizes the species formed during the process but also participates in the reaction assisting the proton transfer between various moieties leading to the formation of carbamic acid.

## Author contributions

Shivam Rawat: data curation, formal analysis, investigation, methodology, and writing – original draft. C. N. Ramachandran: conceptualization, data curation, formal analysis, methodology, project administration, resources, supervision, validation, and writing – review and editing.

## Data availability

The data supporting this article have been included as part of the ESI.<sup>†</sup>

## Conflicts of interest

The authors declare that they have no known competing financial interests or personal relationships that could have appeared to influence the work reported in this paper.

## Acknowledgements

S. R. acknowledges the Council of Scientific & Industrial Research (CSIR), India, for a research fellowship. CNR acknowledges CSIR for the funding (Grant No. 01(2891)/17/EMR-II).

## References

- 1 F. Raganati, F. Miccio and P. Ammendola, Adsorption of Carbon Dioxide for Post-Combustion Capture: A Review, *Energy Fuels*, 2021, **35**, 12845–12868.
- 2 N. El Hadri, D. V. Quang, E. L. V. Goetheer and M. R. M. A. Zahra, Aqueous Amine Solution Characterization for Post-Combustion CO<sub>2</sub> Capture Process, *Appl. Energy*, 2017, **185**, 1433–1449.
- 3 B. Dutcher, M. Fan and A. G. Russell, Amine-Based CO<sub>2</sub> Capture Technology Development from the Beginning of 2013-A Review, *ACS Appl. Mater. Interfaces*, 2015, **7**, 2137–2148.
- 4 M. Zhao, A. I. Minett and A. T. Harris, A Review of Techno-Economic Models for the Retrofitting of Conventional Pulverised-Coal Power Plants for Post-Combustion Capture (PCC) of CO<sub>2</sub>, *Energy Environ. Sci.*, 2013, **6**, 25–40.
- 5 A. Muhammad and Y. Gadelhak, Simulation Based Improvement Techniques for Acid Gases Sweetening by Chemical Absorption: A Review, *Int. J. Greenhouse Gas Control*, 2015, **37**, 481–491.
- 6 U. E. Aronu, H. F. Svendsen, K. A. Hoff and O. Juliussen, Solvent Selection for Carbon Dioxide Absorption, *Energy Procedia*, 2009, **1**, 1051–1057.
- 7 X. Yang, R. C. Rees, W. Conway, G. Puxty, Q. Yang and D. A. Winkler, Computational Modeling and Simulation Of CO<sub>2</sub> Capture by Aqueous Amines, *Chem. Rev.*, 2017, **117**, 9524–9593.
- 8 M. Caplow, Kinetics of Carbamate Formation and Breakdown, *J. Am. Chem. Soc.*, 1968, **90**, 6795–6803.
- 9 G. F. Versteeg, L. A. J. V. Dijck and W. P. M. V. Swaaij, On the Kinetics between CO<sub>2</sub> and Alkanolamines both in Aqueous and Non-Aqueous Solutions, *Chem. Eng. Commun.*, 1996, **144**(1), 113–158.
- 10 J. E. Crooks and J. P. Donnellan, Kinetics and Mechanism of the Reaction Between Carbon Dioxide and Amines in Aqueous Solution, *J. Chem. Soc., Perkin Trans. 2*, 1989, 331.
- 11 N. McCann, D. Phan, X. Wang, W. Conway, R. Burns, M. Attalla, G. Puxty and M. Maeder, Kinetics and Mechanism of Carbamate Formation from CO<sub>2</sub>(aq), Carbonate Species, and Monoethanolamine in Aqueous Solution, *J. Phys. Chem. A*, 2009, **113**, 5022–5029.
- 12 B. Arstad, R. Blom and O. Swang, CO<sub>2</sub> Absorption in Aqueous Solutions of Alkanolamines: Mechanistic Insight from Quantum Chemical Calculations, *J. Phys. Chem. A*, 2007, **111**, 1222–1228.
- 13 J. G. Shim, J. H. Kim, Y. H. Jhon, J. Kim and K. H. Cho, DFT Calculations on the Role of Base in the Reaction between CO<sub>2</sub> and Monoethanolamine, *Ind. Eng. Chem. Res.*, 2009, **48**, 2172–2178.
- 14 E. F. da Silva and H. F. Svendsen, Ab Initio Study of the Reaction of Carbamate Formation from CO<sub>2</sub> and Alkanolamines, *Ind. Eng. Chem. Res.*, 2004, **43**, 3413–3418.
- 15 R. R. Ratnakar, S. Shankar, R. Agrawal and B. Dindoruk, Modeling and Experimental Study on CO<sub>2</sub> Adsorption in Fixed-Bed Columns: Applications to Carbon Capture and Utilization, *J. Nat. Gas Sci. Eng.*, 2021, **94**, 104111.
- 16 E. F. da Silva and H. F. Svendsen, Computational Chemistry Study of Reactions, Equilibrium and Kinetics of Chemical CO<sub>2</sub> Absorption, *Int. J. Greenhouse Gas Control*, 2007, **1**, 151–157.
- 17 J. Schell, K. Yang and R. Glaser, Computational Investigation of the Thermochemistry of the CO<sub>2</sub> Capture Reaction by Ethylamine, Propylamine, and Butylamine in Aqueous Solution Considering the Full Conformational Space via Boltzmann Statistics, *J. Phys. Chem. A*, 2021, **125**, 9578–9593.
- 18 A. Maiti, Atomistic Modeling Toward High-Efficiency Carbon Capture: A Brief Survey with a Few Illustrative Examples, *Int. J. Quantum Chem.*, 2013, **114**, 163–175.
- 19 T. Wang, H. B. Xie, Z. Song, J. Niu, D. L. Chen, D. Xia and J. Chen, Role of Hydrogen Bond Capacity of Solvents in Reactions of Amines with CO<sub>2</sub>: A Computational Study, *J. Environ. Sci.*, 2020, **91**, 271–278.
- 20 M. Narimani, S. A. Iranagh and H. Modarress, CO<sub>2</sub> Absorption into Aqueous Solutions of Monoethanolamine, Piperazine and their Blends: Quantum Mechanics and Molecular Dynamics Studies, *J. Mol. Liq.*, 2017, **233**, 173–183.
- 21 H. B. Xie, X. Wei, P. Wang, N. He and J. Chen, CO<sub>2</sub> Absorption in an Alcoholic Solution of Heavily Hindered Alkanolamine: Reaction Mechanism of 2-(*tert*-Butylamino)ethanol with CO<sub>2</sub> Revisited, *J. Phys. Chem. A*, 2015, **119**, 6346–6353.
- 22 H. Yamada, Y. Matsuzaki, F. Chowdhury and T. Higashii, Computational Investigation of Carbon Dioxide Absorption in Alkanolamine Solutions, *J. Mol. Model.*, 2013, **19**, 4147–4153.
- 23 H. Yamada, F. A. Chowdhury, Y. Matsuzaki, K. Goto, T. Higashii and S. Kazama, Effect of Alcohol Chain Length on Carbon Dioxide Absorption into Aqueous Solutions of Alkanolamines, *Energy Procedia*, 2013, **37**, 499–504.
- 24 M. Ismael, R. Sahnoun, A. Suzuki, M. Koyama, H. Tsuboi, N. Hatakeyama, A. Endou, H. Takaba, M. Kubo, S. Shimizu, C. A. Del Carpio and A. Miyamoto, A DFT Study on the Carbamates Formation through the Absorption of CO<sub>2</sub> by AMP, *Int. J. Greenhouse Gas Control*, 2009, **3**, 612–616.
- 25 S. Kim, H. Shi and J. Y. Lee, CO<sub>2</sub> Absorption Mechanism in Amine Solvents and Enhancement of CO<sub>2</sub> Capture Capability in Blended Amine Solvent, *Int. J. Greenhouse Gas Control*, 2016, **45**, 181–188.
- 26 D. Aso, Y. Orimoto, M. Higashino, I. Taniguchi and Y. Aoki, Why does 2-(2-Aminoethylamino)ethanol have Superior CO<sub>2</sub> Separation Performance to Monoethanolamine? A Computational Study, *Phys. Chem. Chem. Phys.*, 2022, **24**, 14172–14176.



- 27 R. B. Said, J. M. Kolle, K. Essalah, B. Tangour and A. Sayari, A Unified Approach to CO<sub>2</sub>-Amine Reaction Mechanisms, *ACS Omega*, 2020, **5**, 26125–26133.
- 28 M. J. Frisch, G. W. Trucks, H. B. Schlegel, G. E. Scuseria, M. A. Robb, J. R. Cheeseman, G. Scalmani, V. Barone, G. A. Petersson, H. Nakatsuji, X. Li, M. Caricato, A. Marenich, J. Bloino, B. G. Janesko, R. Gomperts, B. Mennucci, H. P. Hratchian, J. V. Ortiz, A. F. Izmaylov, J. L. Sonnenberg, D. Williams-Young, F. Ding, F. Lipparini, F. Egidi, J. Goings, B. Peng, A. Petrone, T. Henderson, D. Ranasinghe, V. G. Zakrzewski, J. Gao, N. Rega, G. Zheng, W. Liang, M. Hada, M. Ehara, K. Toyota, R. Fukuda, J. Hasegawa, M. Ishida, T. Nakajima, Y. Honda, O. Kitao, H. Nakai, T. Vreven, K. Throssell, J. A. Montgomery, Jr., J. E. Peralta, F. Ogliaro, M. Bearpark, J. J. Heyd, E. Brothers, K. N. Kudin, V. N. Staroverov, T. Keith, R. Kobayashi, J. Normand, K. Raghavachari, A. Rendell, J. C. Burant, S. S. Iyengar, J. Tomasi, M. Cossi, J. M. Millam, M. Klene, C. Adamo, R. Cammi, J. W. Ochterski, R. L. Martin, K. Morokuma, O. Farkas, J. B. Foresman and D. J. Fox, *Gaussian 09 (Revision D.01. 2013)*, Gaussian, Inc., Wallingford CT, 2016.
- 29 Y. Zhao and D. G. Truhlar, The M06 suite of density functionals for main group thermochemistry, thermochemical kinetics, noncovalent interactions, excited states, and transition elements: two new functionals and systematic testing of four M06-class functionals and 12 other functionals, *Theor. Chem. Acc.*, 2007, **120**, 215–241.
- 30 T. H. Dunning, Gaussian basis sets for use in correlated molecular calculations. I. The atoms boron through neon and hydrogen, *J. Chem. Phys.*, 1989, **90**, 1007–1023.
- 31 H. C. Li, J. D. Chai and M. K. Tsai, Assessment of Dispersion-Improved Exchange-Correlation Functionals for the Simulation of CO<sub>2</sub> Binding by Alcoholamines, *Int. J. Quantum Chem.*, 2014, **114**, 805–812.
- 32 C. Peng and H. B. Schlegel, Combining Synchronous Transit and Quasi-Newton Methods to Find Transition States, *Isr. J. Chem.*, 1993, **33**, 449–454.
- 33 A. E. Reed, L. A. Curtiss and F. Weinhold, Intermolecular Interactions from a Natural Bond Orbital, Donor-Acceptor Viewpoint, *Chem. Rev.*, 1988, **88**, 899–926.
- 34 R. F. W. Bader, Atoms in Molecules, *Acc. Chem. Res.*, 1985, **18**, 9–15.
- 35 T. Lu and F. Chen, Multiwfn: A Multifunctional Wavefunction Analyzer, *J. Comput. Chem.*, 2011, **33**, 580–592.
- 36 W. Humphrey, A. Dalke and K. Schulten, VMD: Visual molecular dynamics, *J. Mol. Graphics*, 1996, **14**, 33–38.
- 37 S. Grimme, Semiempirical hybrid density functional with perturbative second-order correlation, *J. Chem. Phys.*, 2006, **124**, 34108.
- 38 S. Grimme, S. Ehrlich and L. Goerigk, Effect of the damping function in dispersion corrected density functional theory, *J. Comput. Chem.*, 2011, **32**, 1456–1465.